Ground motion and PSI density analysis from Envisat and Sentinel1a InSAR data in the context of a complex landslide monitoring strategy in Karnali river basin, Far-Western Nepal

Filippo Vecchiotti[1] ,Arnulf Schiller[1],Anna Sara Amabile[1], Carlotta Guardiani[1], Megh Raj Dhital[2], Amrit Dhakal[2], Bharat Raij Pant[2], Marc Ostermann[1], and Robert Supper[1]

[1] GBA - Geological Survey of Austria; [2] Tribhuvan University Kathmandu

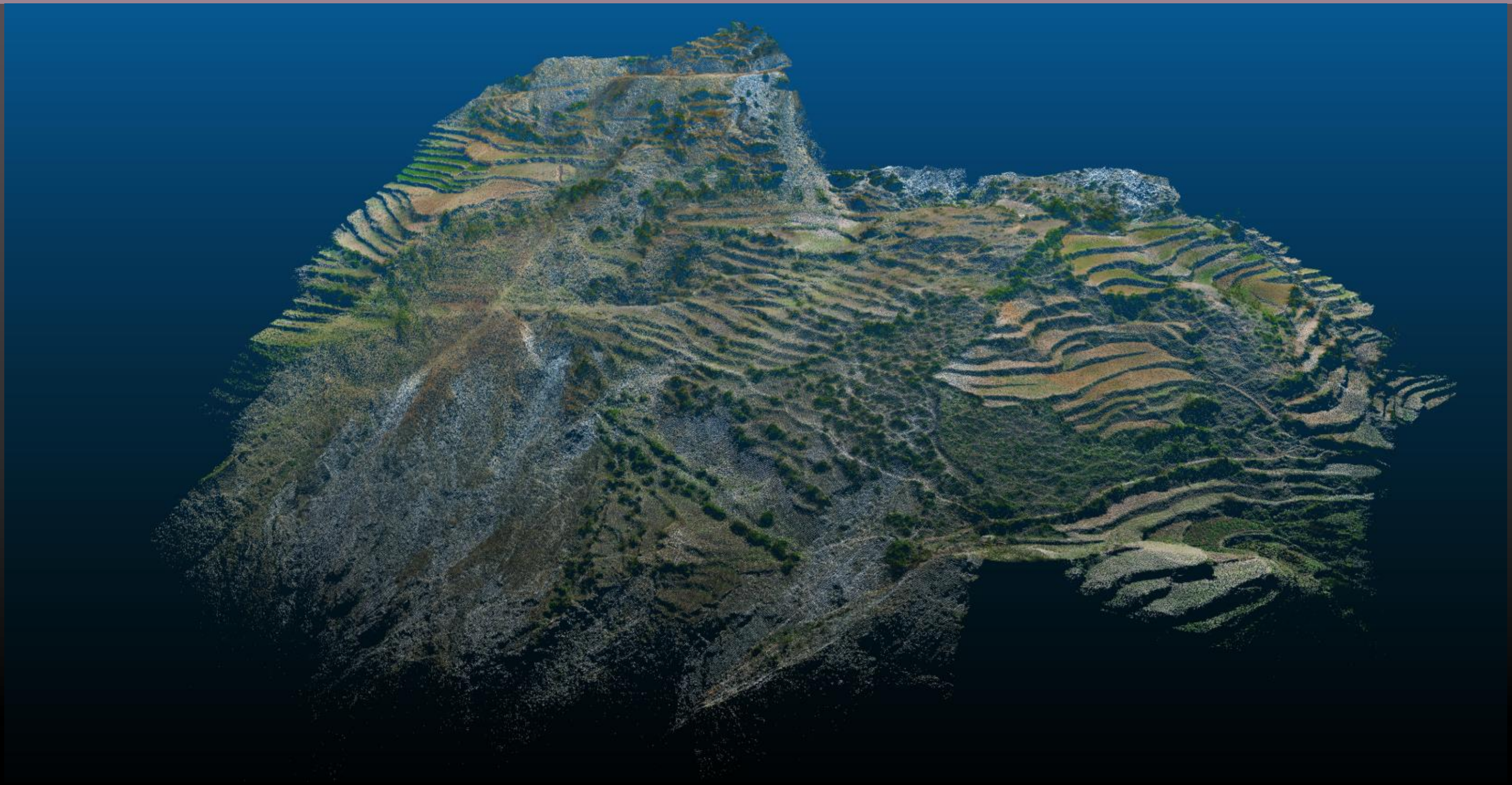

Contents

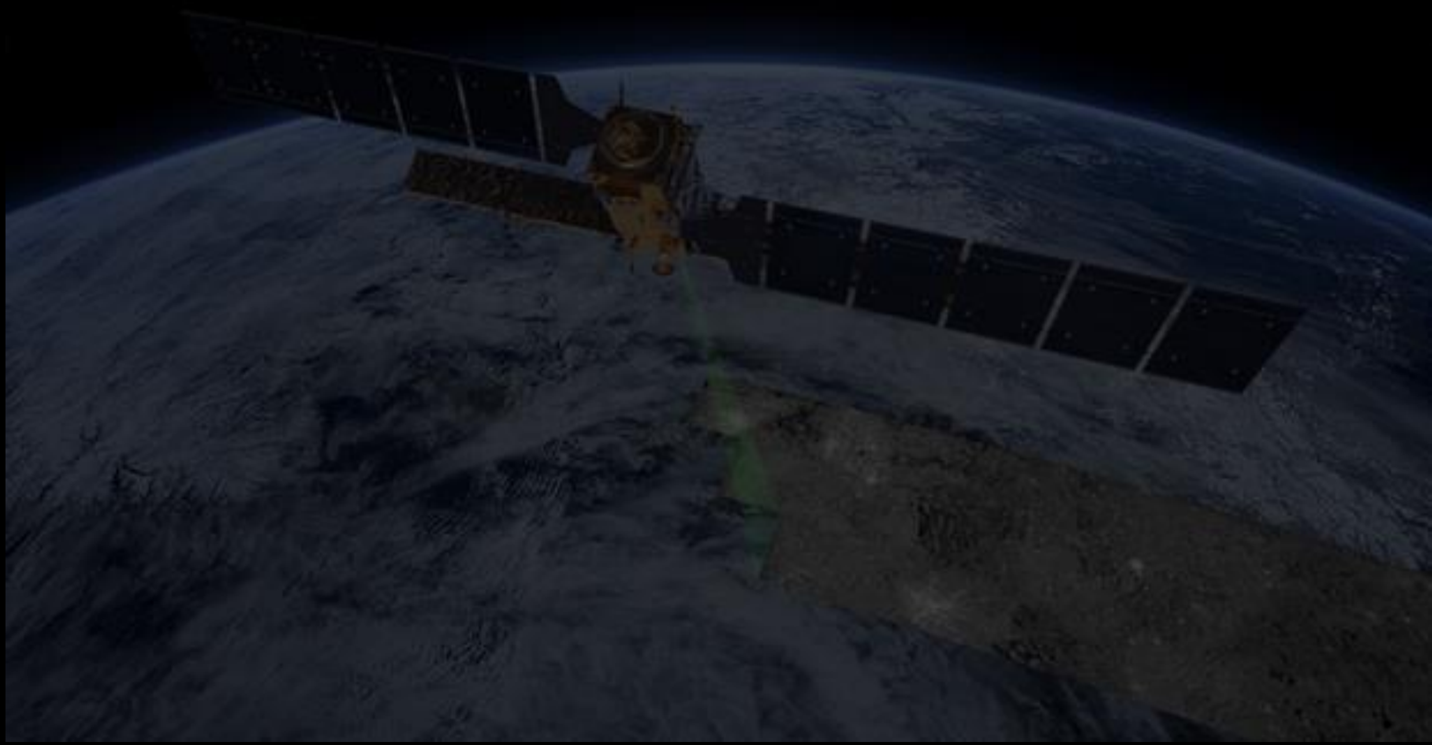

This document contains complementary material concerning our contribution to the EGU General Assemby 2020, May 4-8 online, taking place in World Wide Web due to the Covid-19 pandemy. The content addresses geoscientists and institutions of different expertise and does not represent a final publication (which is intended). The authors would appreciate to be contacted in case of further use of the material. Contact: arnulf.schiller@geologie.ac.at

Context

DInSAR as part of a complex regional and Local landslide monitoring approach in framework of the project 'Landslide-EVO'

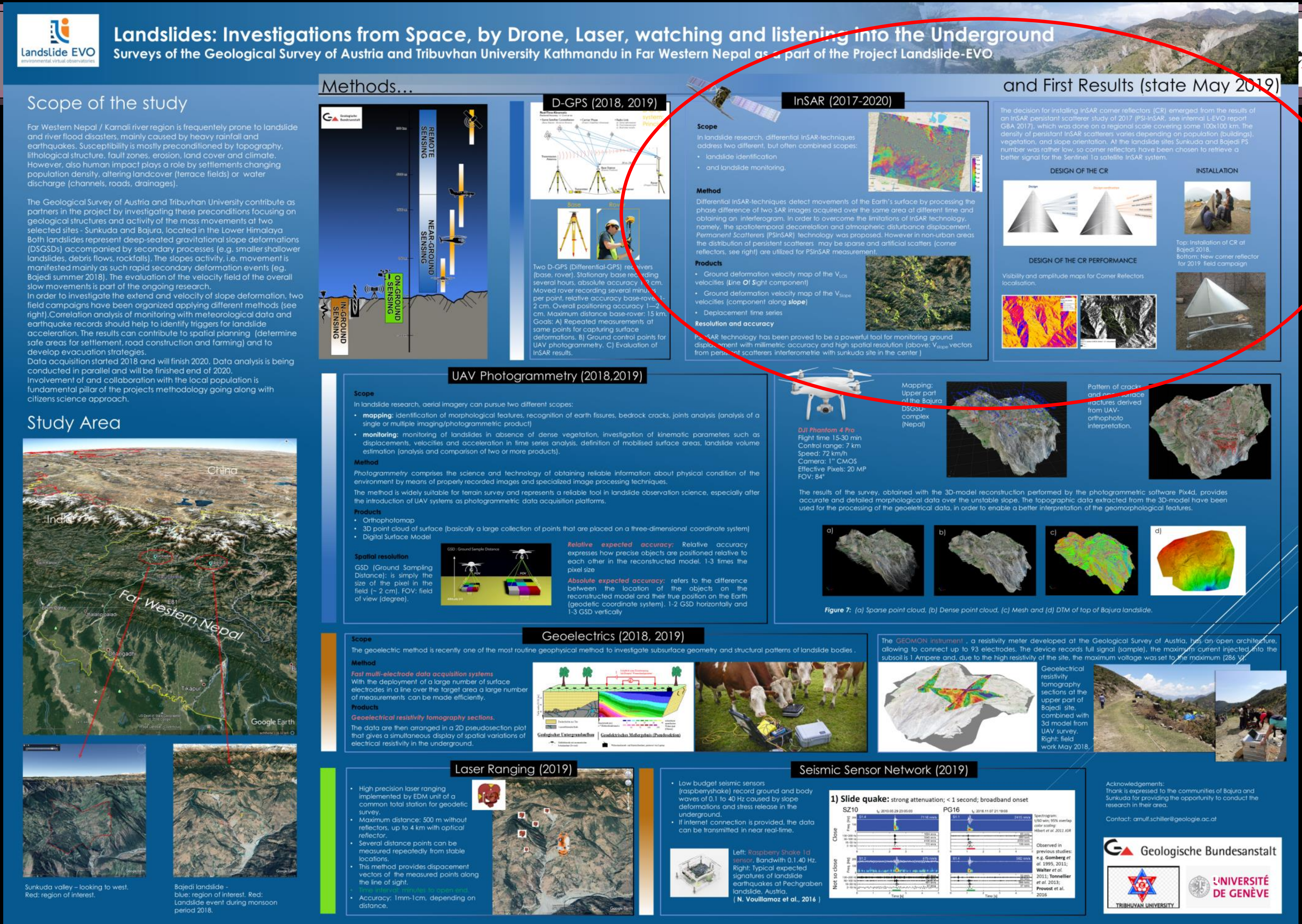

Duration: 2017-2021,

SHEAR funded, lead:

Imperial College London.

http://www.shear.org.uk/research/landslide-evo.html

Objectives of the study

Preparation of

- PSI a priori visibility map
- PSI density map
- Multi-Temporal-DInSAR deformation maps
- ‘Spin off products’ (e.g. ground instability map)

Scale:

- Regional: Far Western Nepal
- Local: Bajedi (monitoring system), Sunkuda

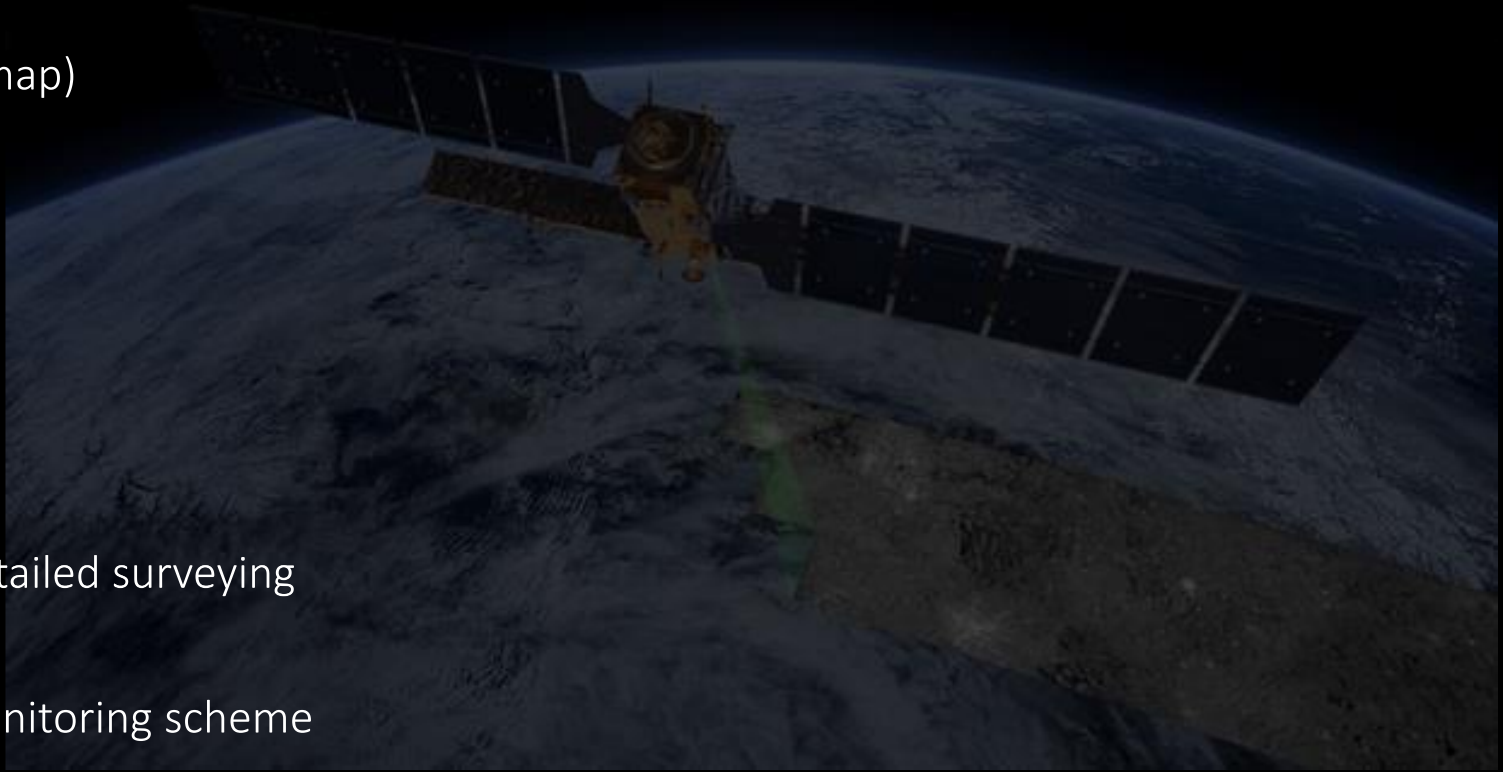

Purpose:

- Support in selection of landslide sites for detailed surveying and monitoring
- Support in planning and part of complex monitoring scheme
- Data base for supporting decision processes for adaption to landslide risk on local and regional level.

Methodology

A) Reviewing available data ressources (DEM, geographical, landcover, geomorphology, geology and tectonics, climatology and meteorology, remote sensing - INSAR)

B) Selection and implementation of feasible software (ArcGIS, GRASS GIS, QGIS, SAGA, Orfeo, Phyton plugins and remote sensing services)

C) Generation of a priory PSI visibility map (RI-index)

D1) Generation of a priory PSI density map (RI-index combined with landcover classes OSM data)

D2) Reviewing, test and selection of methods (multitemporal DInSAR/PSI-InSAR, SBAS)

D3) Corrections/filtering specific to distinct topography and atmospheric conditions

E) Deriving deformation rates (along line of sight - VLOS , along slope - VSLOPE)

F) Accompanying: Compilation of maps of ground instability and landslides

Use of the ENVISAT data for the multi-temporal InSAR methods

Differential InSAR (DInSAR) techniques can detect movements of the Earth's surface with sub-millimetric precision.

The radar information acquired by the satellites and used for InSAR processing consist in the amplitude and the absolute phase images of the reflected radar signal.

Through the InSAR technique, the phase difference (Interferogram) between two SAR images is calculated and converted into displacements along the range direction or LOS, which occurred in the time between two SAR images acquisitions.

In order to overcome the limitations of DInSAR, namely the spatio-temporal decorrelation and atmospheric disturbance displacement, MT DInSAR techniques were proposed, including two approaches—persistent scatterers interferometry (PSI) and small baseline subset (SBAS).

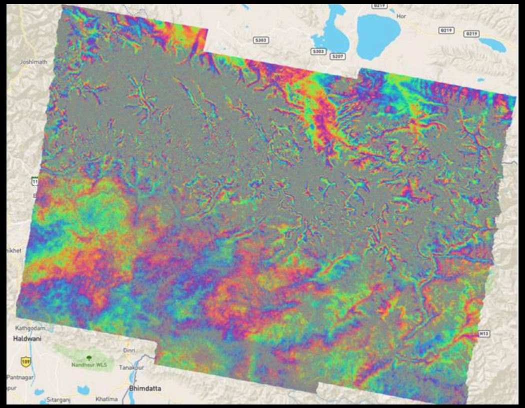

Example interferogram of Far Western Nepal region.

Persistent Scatterers In SAR (PSI)
Standard PSI technique processes all interferograms with respect to same master image. No spectral filtering is applied in order to maximize full resolution and an a priori DEM is used for evaluation of the residual topography and minimize phase ambiguities.

Small Baseline Subset InSAR: SBAS uses a network of redundant interferograms with no need to use a unique master scene:

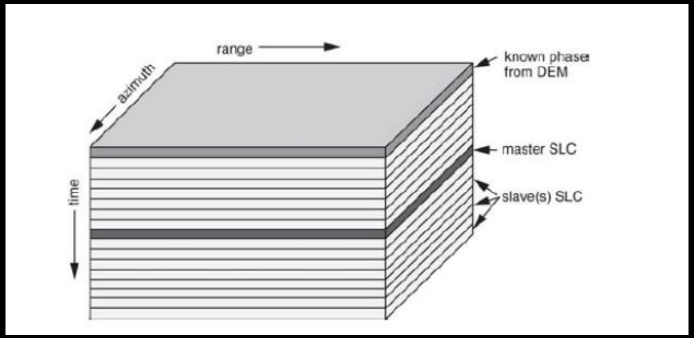

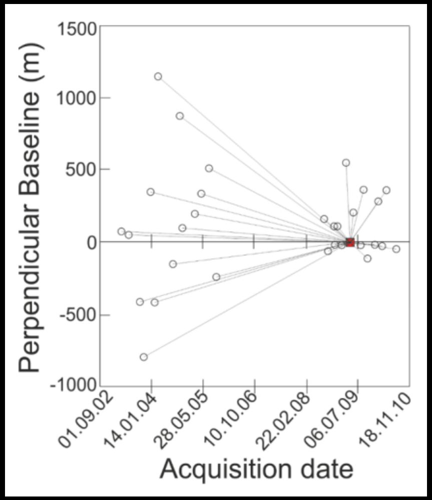

Top: Use of Envisat multitemporal InSAR data: Schematic diagram of a stack of SAR images (from Sandwell et al. 2011).
Right: Identification of the master (21.04.2009) image in red and the interferogram stack used for the PSI processing of track 205

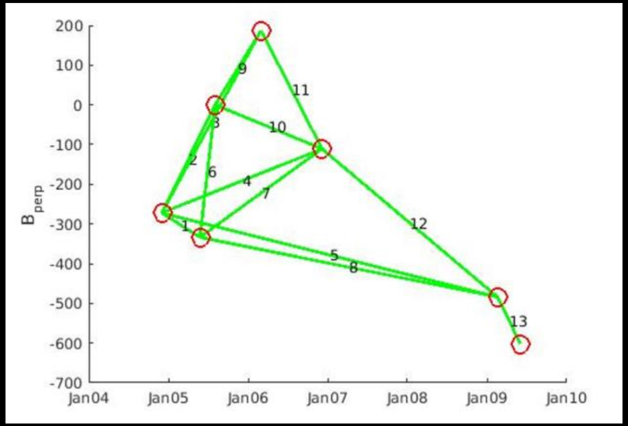

Network of 13 interferograms used for SBAS processing of track 55.

Generation of Priori Visibility Map and PSI Density Map

The "***a priori PSI visibility map***" for far western Nepal was generated in order to evaluate the feasibility of Differential SAR Interferometric (DInSAR) applications for landslide-affected slopes.
The a priori PSI visibility map is useful to forecast which areas are expected to be visible from space-borne SAR sensors (Cascini et al., 2010). This method helps to predict the density of the Persistent Scattereres PS (the targets for each satellite) and therefore facilitates to select the image dataset over the areas of interest for monitoring.
The factors determining the visibility of target area of a slope are: 1) the orientation of the employed satellites Line-Of-Sight (LOS) and 2) the radar acquisition geometry with respect to the local slope orientation and aspect. DEM data from TanDEM-X (TerraSAR-X add-on for Digital Elevation Measurement) and the ASTER DEM 30m were used.

$$RI = -\sin(S * \sin(A+\varphi)-\vartheta)$$

S = local terrain slope
A = aspect angle
φ = orientation angle
ϑ = incidence angle

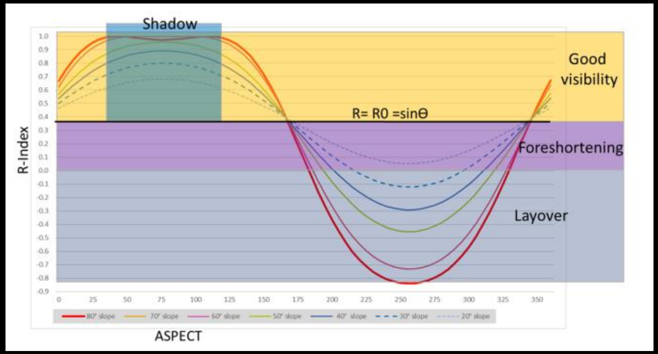

The a priori visibility maps are calculated for the following SAR sensors:
- [C-band] ERS-ENVISAT, RADARSAT and SENTINEL-1 (S1);
- [L-band] ALOS PALSAR;
- [X-band] CosmoSkyMed (CSK) and TerraSAR-X (TSX).

The "***a priori PSI density map***" for East western Nepal was generated in order to evaluate the feasibility of MT-InSAR applications for landslide affected slopes.
The factors that determine the quantity of PS per unit area are:
- the a priori PSI visibility map based on RI index
- land cover map, thus vegetation cover and presence of building and other infrastructures (pylons, railways, etc.), rock and debris (Cigna et al., 2014).

The presence of stable reflectors in the ground surface can be estimated from the land cover map. Therefore, the integration of *land cover* data in the *proposed geometrical model (a priori visibility map)* can improve the prediction of those areas where PS maybe detected (Notti et al. 2014).

Data resources for land cover: Globcover global land cover map, OpenStreetMap.

Overview of the PS density values assigned to each new land cover class

method	corine	new land cover	class code	ENVISAT & ERS (PS/km^2)	Radarsat (PS/km^2)	Alos Palsar (PS/km^2)	CosmoSkyMed (PS/km^2)	TerraSAR-X (PS/km^2)	Sentinel-1 (PS/km^2)
Unique value	335	glacier	class1	0	0	0	0	0	0
averaged	211-221-242	crop	class2	28	33	108	24	30	90
avgeraged	311-313	forest	class3	8	9	44	0	0	23
Unique value	324	shrub	class4	10	12	76	36	45	30
averaged	321-322	grass	class5	64	73	287	83	104	190
Unique value	332	bare land	class6	100	115	382	722	903	300
Unique value	112	urban	class7	600	693	688	4330	5419	1800
avgeraged	511-512	water	class8	0	0	0	0	0	0
Unique value	122	roads	class10	320	369	382	2309	2890	960

Generation of Deformation / Velocity Maps

Extraction of the deformation rate along the slope (Vslope)

Displaysment measurement of PSI and SBAS methods are calculated along the LOS. In order to retrieve VSLOPE a conversion is needed. Since normally we are not dealing with flat terrains if the LOS measurement in 3D wants to be exploited a projection along the slope is requires. The LOS projection of deformation can be obtained as the scalar product of 3D displacement v velocity and the so-called sensitivity versor u whose components highlight the impact of both horizontal (easting and northing) and vertical phenomena on the LOS measurement carried out by the SAR system(Colesanti and Wasowski, 2006). The LOS of ENVISAT satellite in ascending mode is characterized by the azimuth (α) = 260.7° which expresses the angle between the N and the negative direction of the LOS vector and look angle (β) = 23.4° .

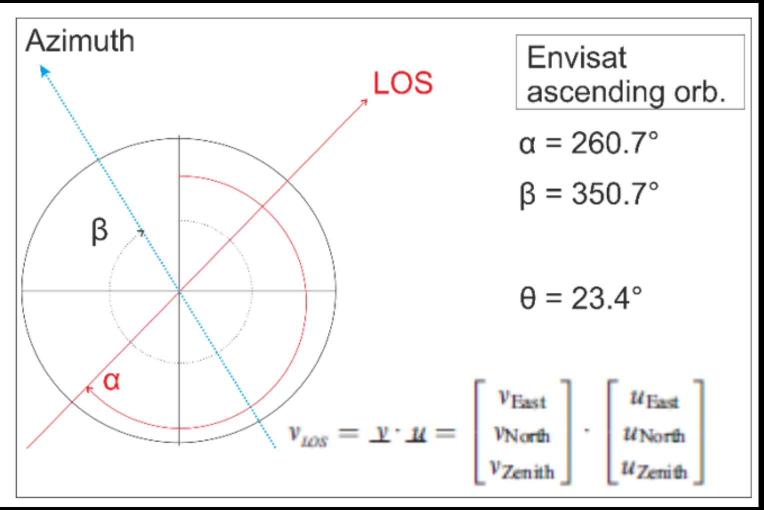

Geometrical characteristics for ENVISAT in ascending mode. α, azimuth; β , tilt (measured between LOS and horizontal direction); θ look angle (measured between LOS and vertical direction).

VSLOPE: Projection of VLOS onto slope gradient direction

ELOS = sinα * cosβ
NLOS = cosα * cosβ
ZLOS = sinβ

VSLOPE =ρ * VLOS with ρ = (ELOS * ESLOPE + NLOS * NSLOPE + ZLOS * ZSLOPE)-1

ELOS, NLOS and ZLOS values represent the percentages of the real motion that it is possible to estimate along the 3 direction E-W, N and vertical. Normally for the modelling of the LOS results, we adopt a simplified geomorphologic scheme where the motions affecting the areas are assumed to be purely translational along the instable slope. In this way, the LOS deformation vector in both ascending and descending mode (VLOS) is converted in VSLOPE in order to represent the motion along the steepest slope direction (Cigna et al. 2011, Cascini et al. 2010). The conversion to slope velocity was performed for each group of pixels using the following equations:

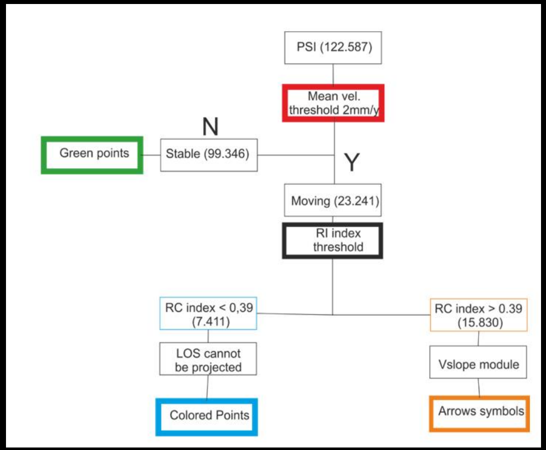

Flow-chart for the generation of the advanced combined VSLOPE and VLOS landslide velocity map for the SBAS method applied to the track 205 descending (modified after Cascini et al. 2010).

Results: PSI Visibility Maps

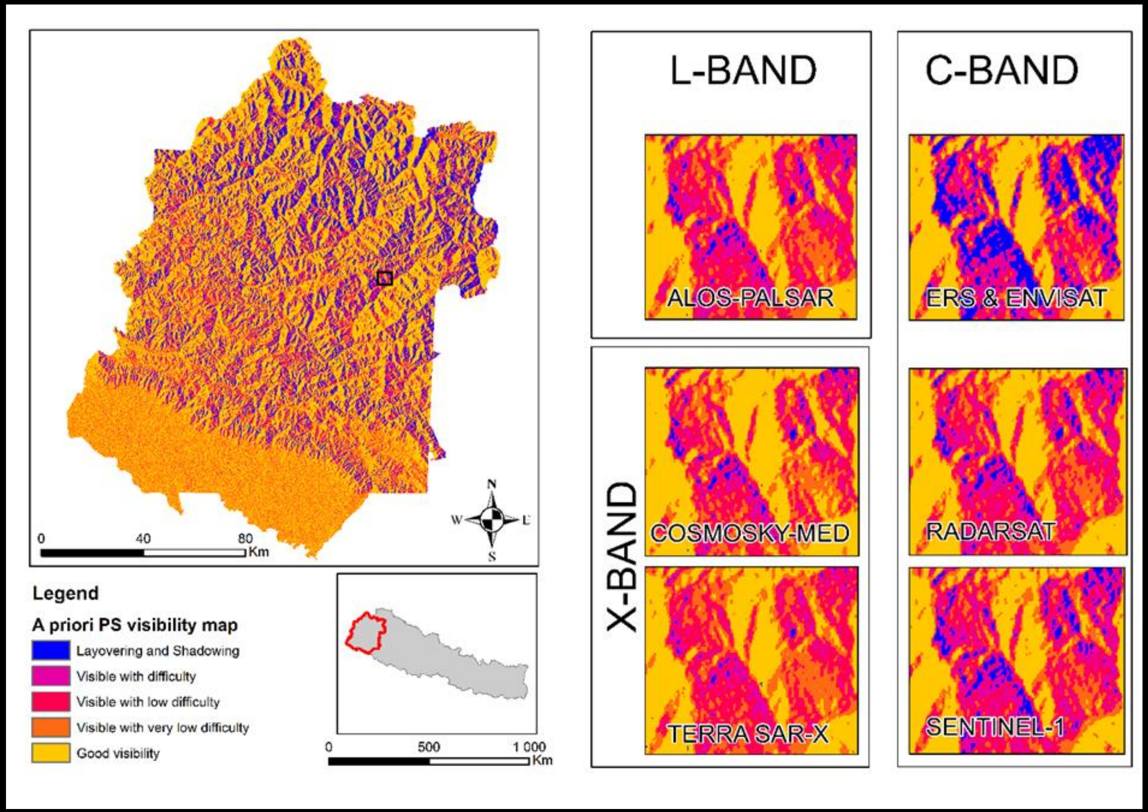

A priori PS visibility map for descending geometry (30m resolution) for the whole region of interest and representation of a close look at the Bajedi basin to allow for a satellite inter-comparison.

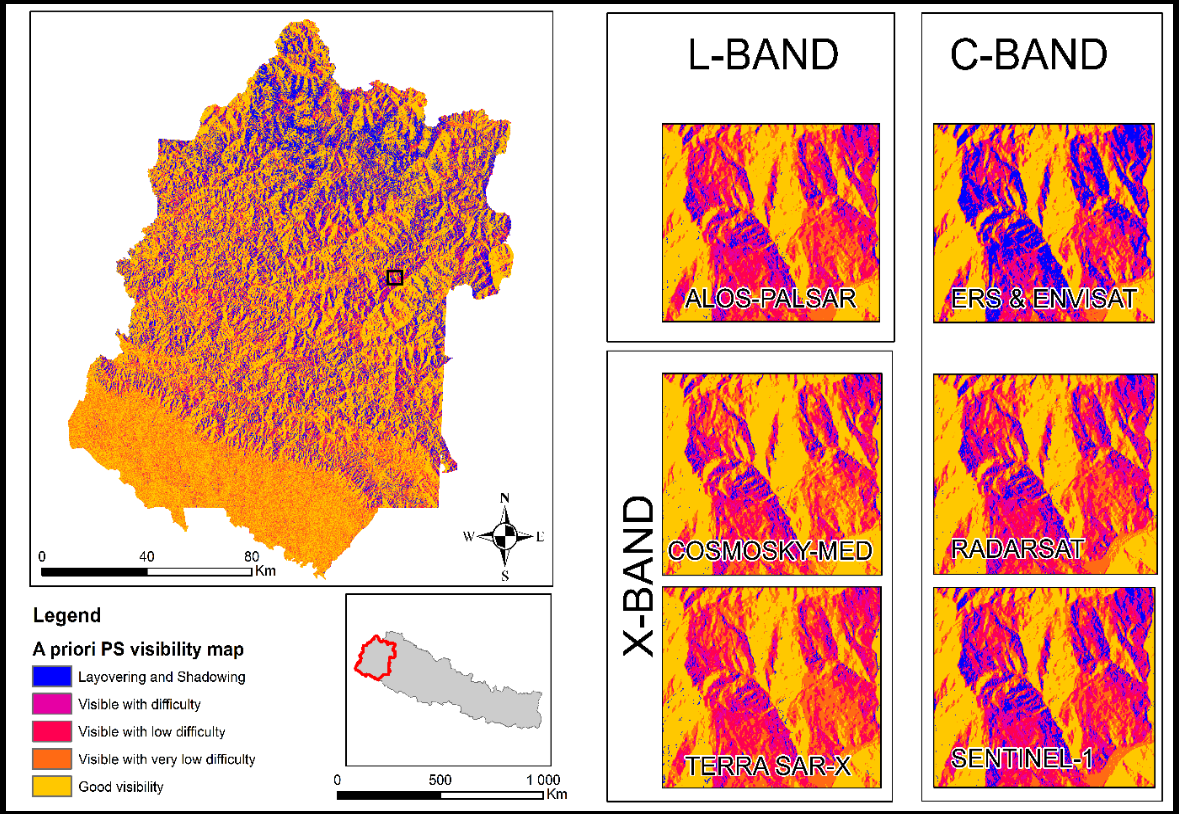

A priori PS visibility map for descending geometry (12m resolution) for the whole region of interest and representation of a close look at the Bajeda basin to allow for a satellite inter-comparison.

Results: PSI Visibility Maps

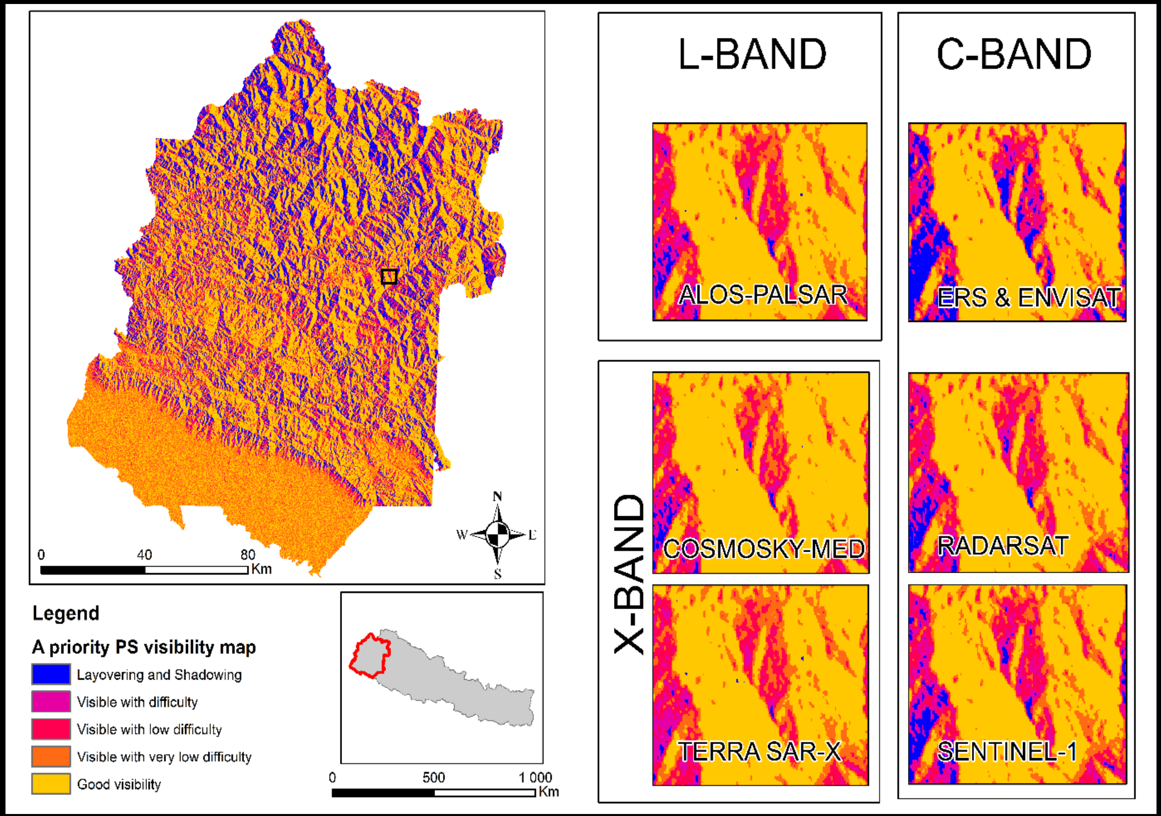

A priori PS visibility map for ascending geometry (30m resolution) for the whole region of interest and representation of n close look at the Bajeda basin to allow for a satellite inter-comparison.

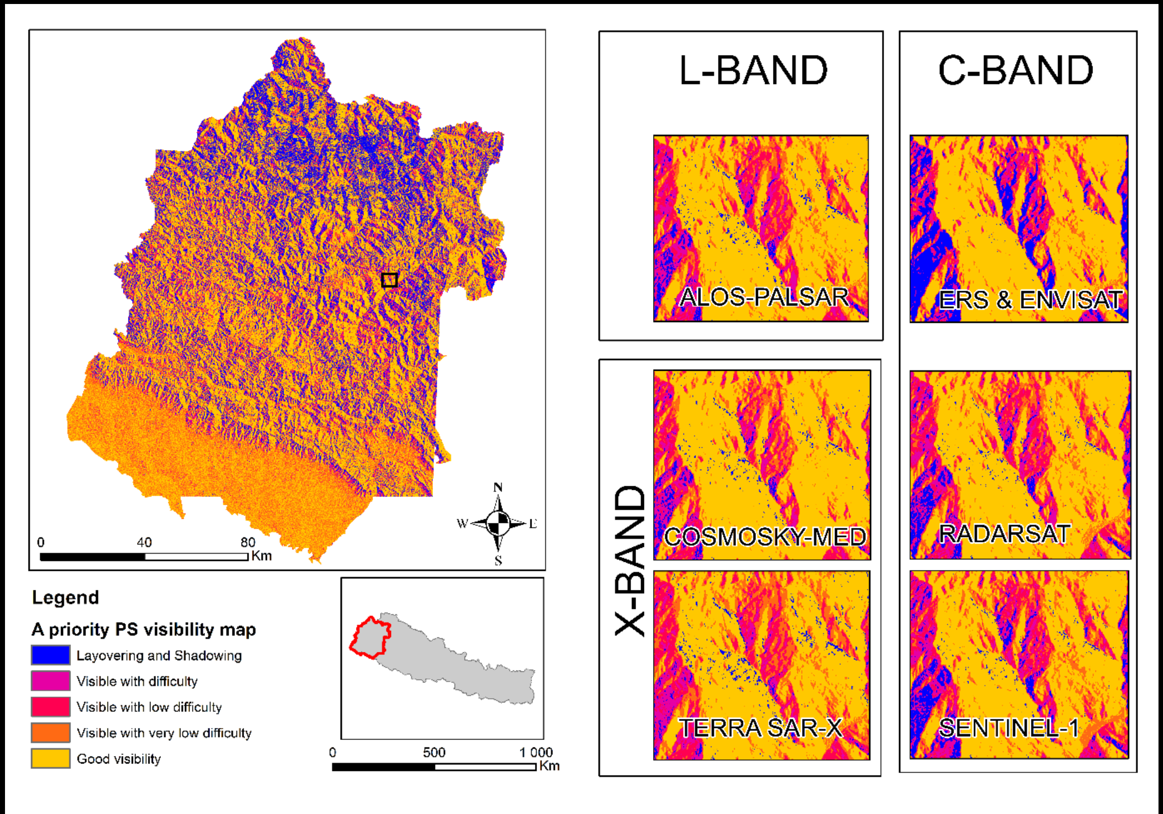

a priori PS visibility map for ascending geometry (12m resolution) for the whole region of interest and representation of a close look at the Bajeda basin to allow for a satellite inter-comparison.

Results: PSI Density Maps

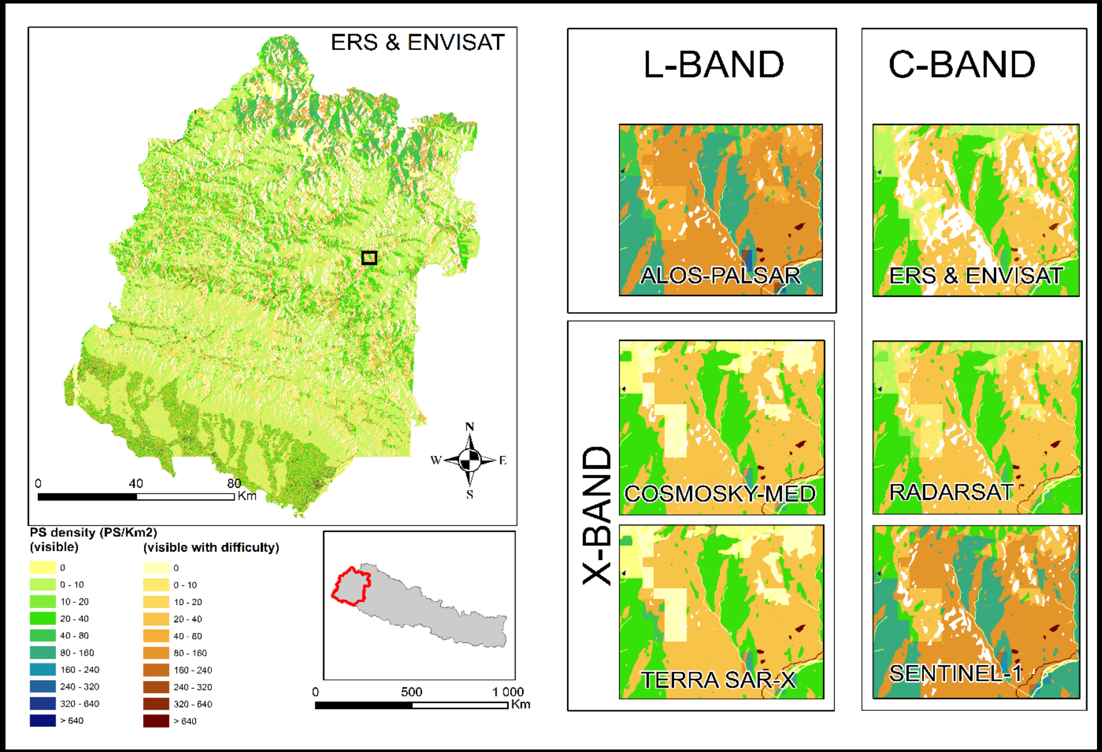

A priori PS density map for descending geometry for the whole region of interest and representation of a close look at the Bajeda basin to allow for a satellite inter-comparison.

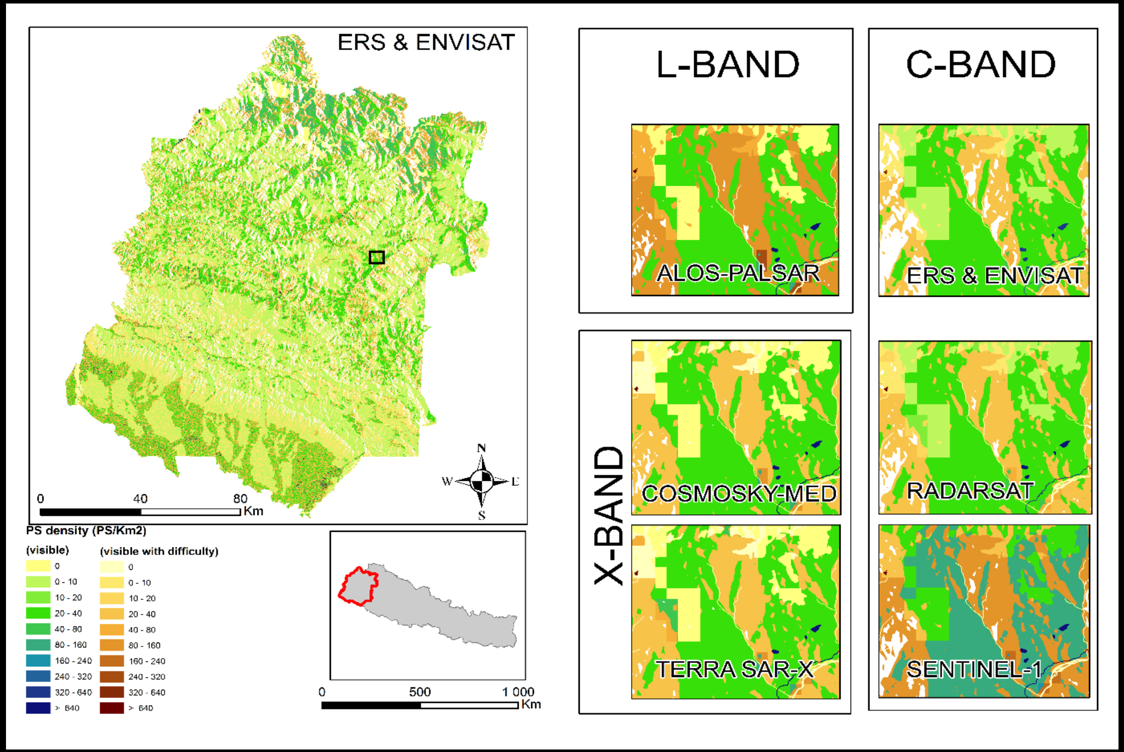

A priori PS density map for ascending geometry for the whole region of interest and representation of a close look at the Bajeda basin to allow for a satellite inter-comparison.

Results: Ground deformation maps SBAS - method

Final SBAS deformation map for track 205 in the time interval 2003-2010 expressed in VSLOPE (oriented arrows).

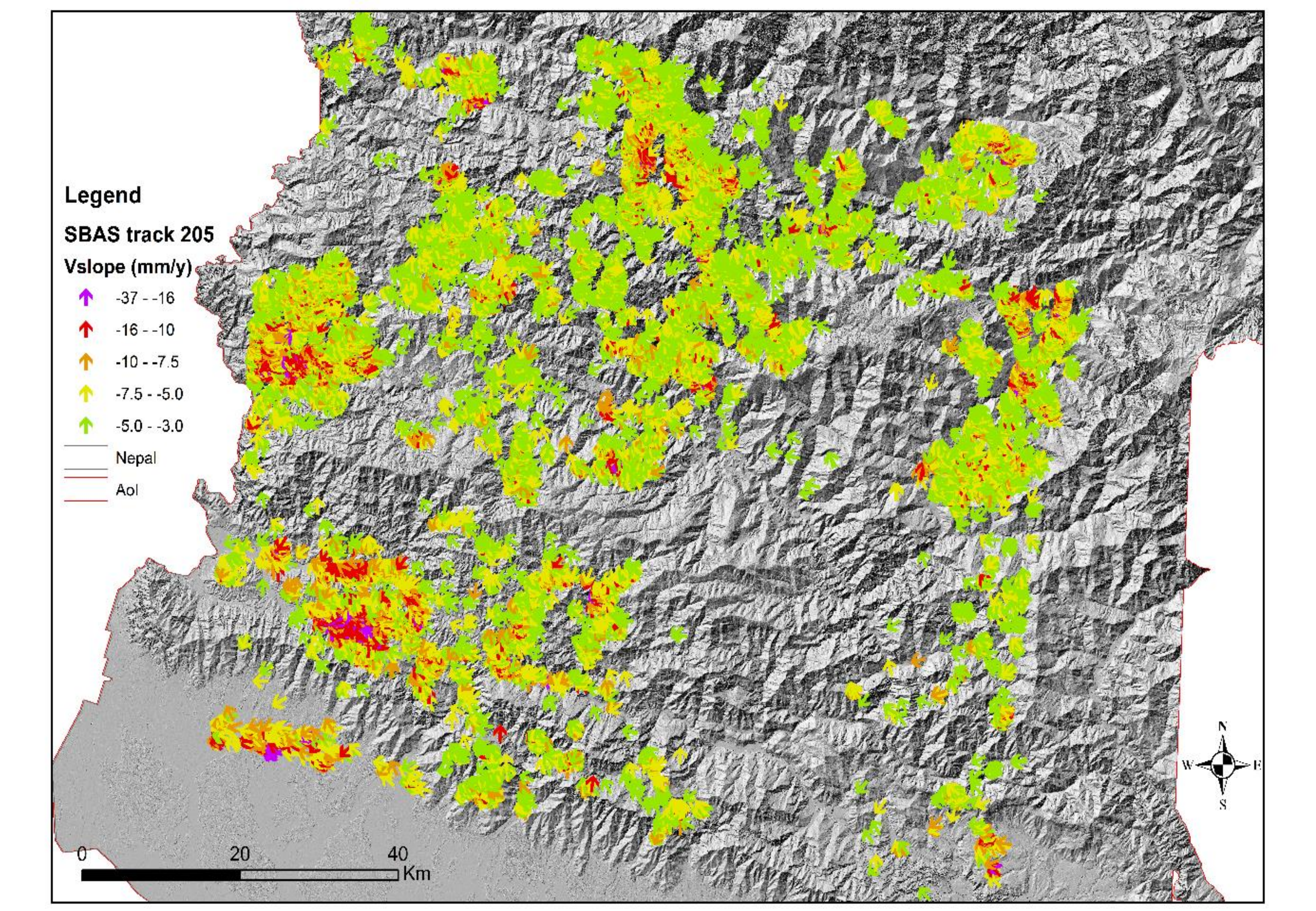

Results: Ground deformation maps – PSI method

Final PSI deformation map for track 205 in the time interval 2003-2010 expressed in VSLOPE (oriented arrows).

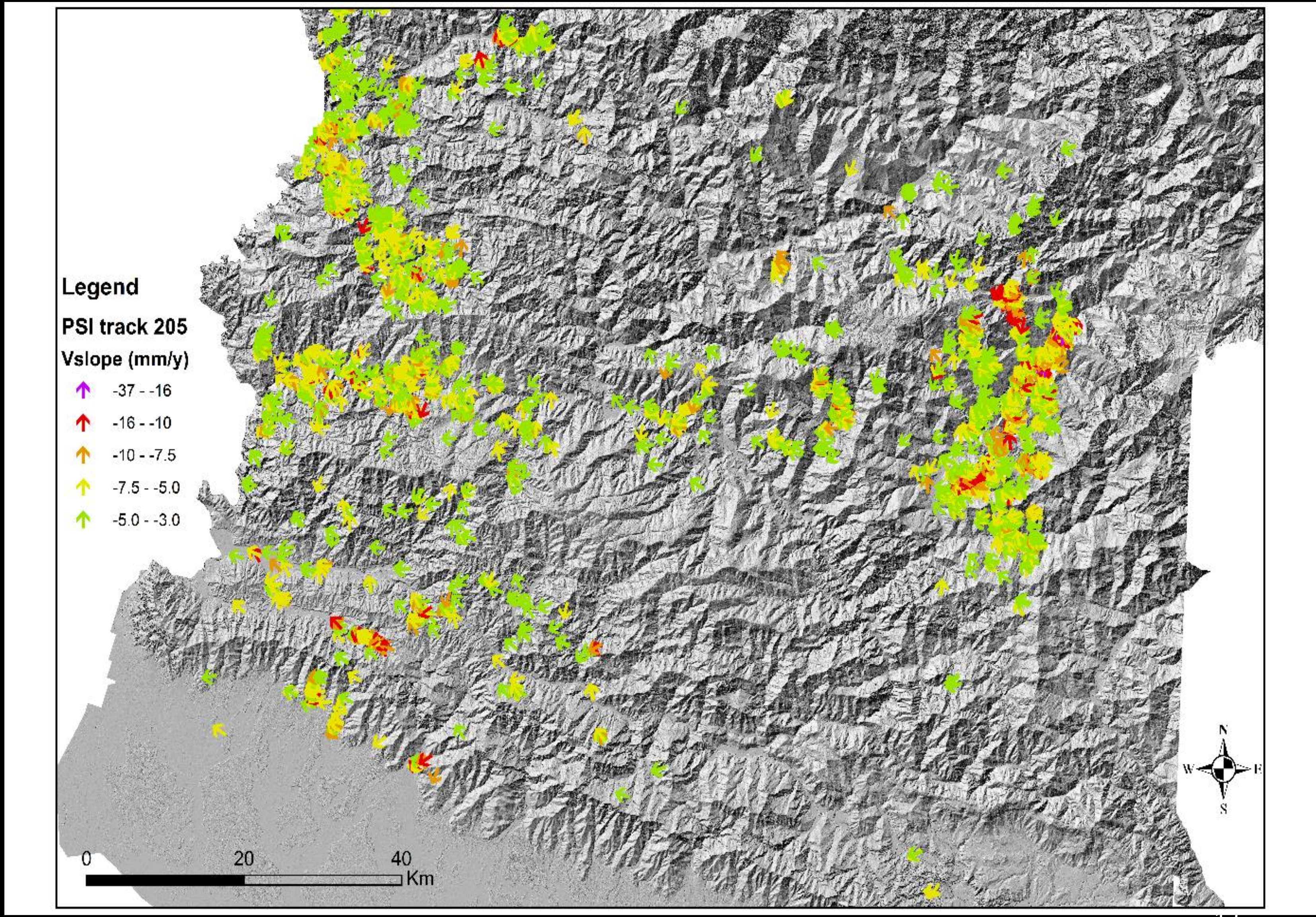

Local Scale: Deep Seated Gravitational Slop Deformations (DSGSDs) at Sunkuda and Bajura

Different type of gravitational mass movements are widespread in the mountain region of Nepal. Additionally the middle altitudes areas show an uncommon high population density and large parts of the slopes are used for agriculture. Therefore, the risk to get affected by landslides is one of the highest in the world.

The Geological Survey of Austria (GBA) and the Tribhuvan University Kathmandu contribute as partners in the project Landslide-EVO (2017-2021) with the task to characterize and monitor two active Deep Seated Gravitational Slop Deformation **(DSGSDs)** at Sunkuda and Bajura (Bajedi, Fig. bottom). Both sites are located in the Karnali river basin, Lower Himalaya of Far Western Nepal. The DSGSDs there are accompanied by secondary processes like shallow landslides, debris flows and rock falls.

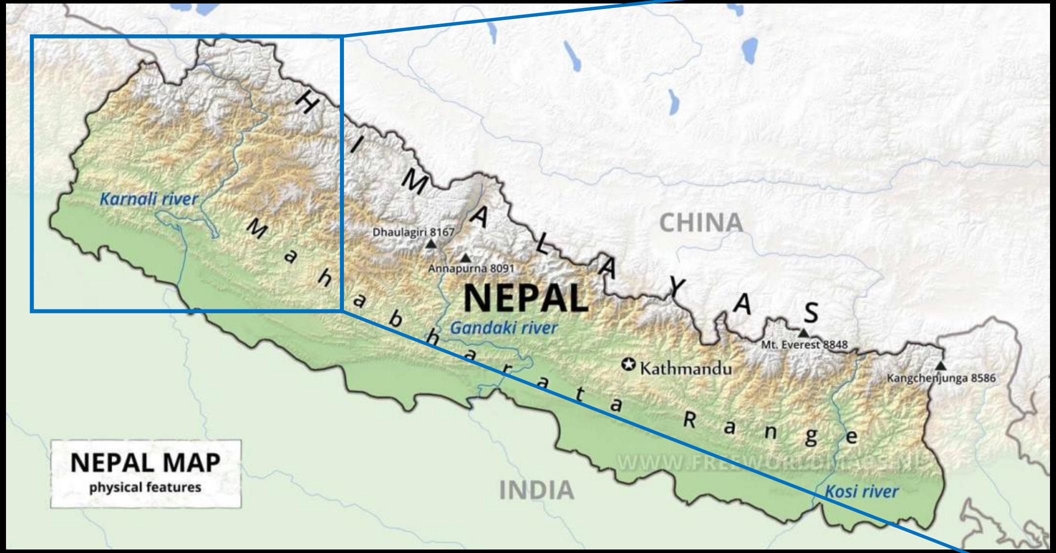

Location of the Deep Seated Gravitational Slop Deformations at Sunkuda and Bajura

Catchment Scale: Bajedi (Bajura) Landslide

A first investigation around the area of the Bajeda catchment and Budiganga river basin was performed in terms of Deep Seated Gravitational Slope Deformation (DSGSD) phenomena recognition based only on geomorphologic interpretation. A DSGSD database was created and from Budiganga river basin in the figure bottom left two types of mass movement were represented:

- In orange the optical images interpreted active shallow landslides
- In red the DSGSD interpreted via geomorphology evidences.

When these polygons are overlaid to the ascending SBAS data, a first impression of how to create a landslide activity map can be given (bottom right).

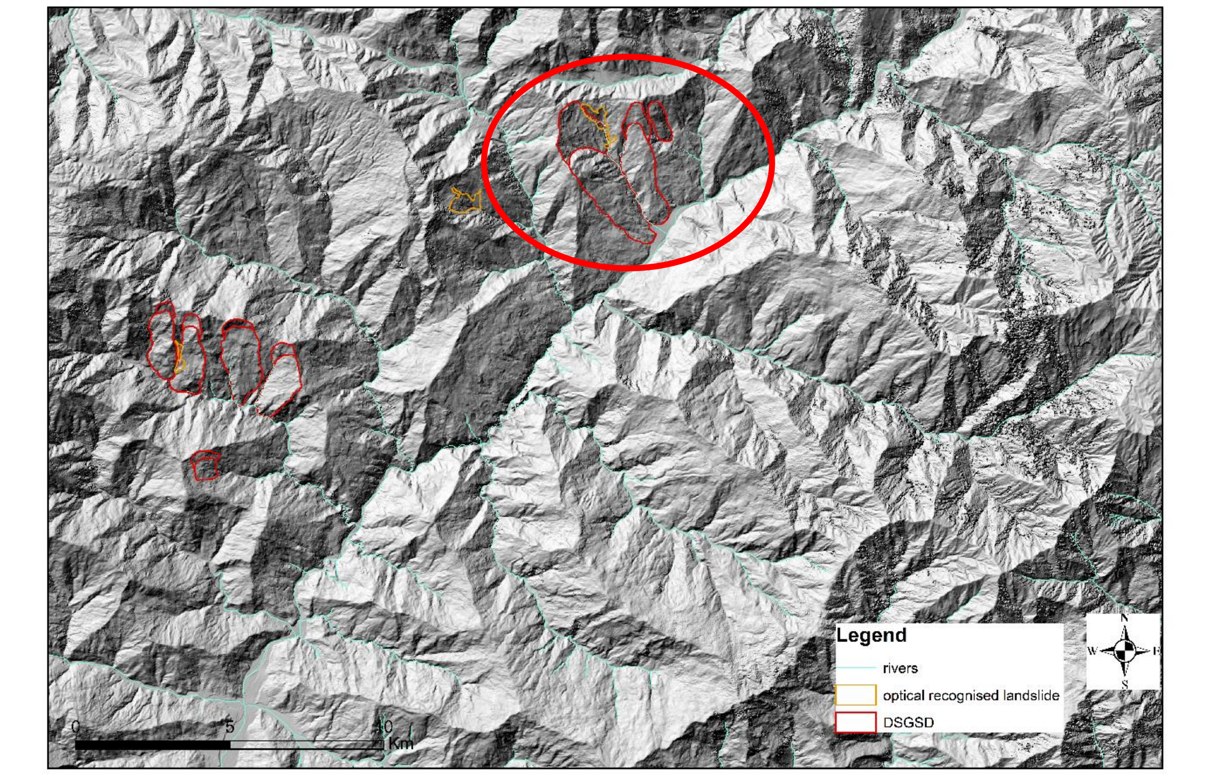

Preliminary identified superficial (in orange) and deep seated (in red) landslides around the area of the Bajeda catchment and Budiganga river basin

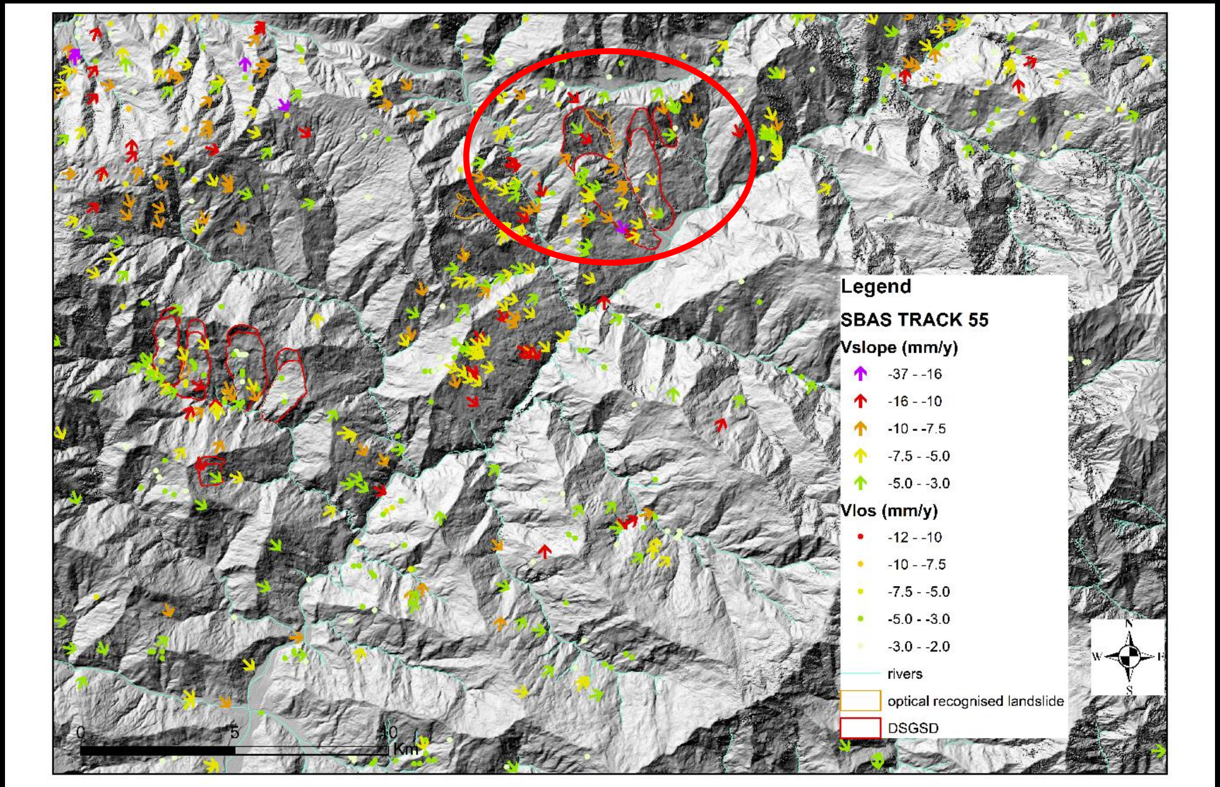

VLOS and VSLOPE vectors for ascending orbit (suitable for west oriented slopes) around the area of the Bajeda catchment and Budiganga river basin.

Conclusion and Recommendations

Multi-Temporal DInSAR technique as developed in Austria is succesfully applied to Far Western Nepal

Semi-automatic process flow in GIS environment yields a priori PS visibility and density maps on basis of existing or free available DEM (ASTER 30m, TerraSAR, ALOS world 3D).

A priory visibility map supports accurate positioning of InSAR-corner reflectors for punctual InSAR-monitoring (Bajedi).

Higher resolution (at least 30m) landcover map for Far Western Nepal would improve PSI-density information.

Multisensor MT-DInSAR: Use of multiple sensors enables derivation of multiple velocity fields and denser time series for monitoring (combining L, C, X-band sensors, different revisiting times, ERS, ENVISAT, ALOS, Cosmo-Sky_Med, Sentinel-1).

Current pallette of applied free data ressources and services/ software allows low cost implementation of DInSAR monitoring (see references).

Nepal partners and institutions can realize such monitoring on regional and catchement scale throughout the state and beyond runtime of the project supporting effective risk managment, early and selective and reaction to landslide risk.

The Geological Survey of Austria is ready to support and transfer developed expertise to Nepal partners (e.g.: Workshop ‚Landslide Monitoring Systems and Methods‘, November 2019, Vienna).

Acknowledgement

Thank is expressed to the partners of Tribhuvan University, Practical Action Consulting and SOHAM for providing most actual data and on site logistics also to the citizens of Bajedi and Sunkuda community for local support, the Austrian and Nepal Ministry for Foreign Affairs, the Austrian Embassy New Delhi, as well as the Austrian Honorary Consulate Kathmandu for logistics and administrative support concerning equipment shipping.

landslide EVO
environmental virtual observatories

THANKS FOR YOUR ATTENTION

Data ressources, processing platforms and applied software

Digital elevation models
Three different digital models available at the time were used for the project.
a 30 m ASTER (Advanced Spaceborne Thermal Emission and Reflection Radiometer) Global Digital Elevation Model (ASTER DEM) released in 2011 by the Ministry of Economy, Trade, and Industry (METI) of Japan and the NASA.
12 m DEM TanDEM-X (http://sss.terrasar-x.dlr.de/).
Nasa SRTM 90m resolution DEM for the interferometric process (http://www.cgiar-csi.org/data/srtm-90m-digital-elevation-database-v4-1)

Geographical
Airports (https://data.humdata.org/organization/ocha-nepal)
Disaster data (https://data.humdata.org/organization/ocha-nepal)
geography at 5 sub national level (https://data.humdata.org/organization/ocha-nepal)
Population (http://www.diva-gis.org/gdata)

Land cover
Globcover global land cover map (http://due.esrin.esa.int/page_globcover.php)
OpenStreetMap layers including rivers, lakes, point of interests, village and cities buildings (http://download.geofabrik.de/asia/nepal.html)

Geomorphology
Soil map from Soter Project (http://data.isric.org/geonetwork/srv/eng/catalog.search#/metadata/896e61f8-811a-40f9-a859-ee3b6b069733)
Physiographic region (partner data)
World landslide database (https://data.nasa.gov/Earth-Science/Global-Landslide-Catalog/h9d8-neg4/data)
Wathershed and Rivers extraction (DEM derived via GRASS GIS)
Geomorphon (DEM derived via GRASS GIS)
Skyview factor (DEM derived via GRASS GIS)
Contour lines and Hillshades (DEM derived via ArcGIS)

Remote sensing
ESA ENVISAT SLC data 31 descending and 9 ascending track number 55 and 7 ascending track number 327 (in table 1,2 and 3 the major characteristics of the image are summarized).
(SNAP http://step.esa.int/main/toolboxes/snap/) is already tested and used at the Geological Survey of Austria. Data is generally freely available from servers (https://scihub.copernicus.eu/dhus/#/home) or provided after short project application (https://geohazards-tep.eo.esa.int; OSEO - open Science Earth Observation- call from ESA https://earth.esa.int/web/guest/home).

Geology and tectonics

Geology of Nepal, Active Faults scale 1: 1000.000 (Dithal, 2015).

Geology of Nepal scale 1:2000.000 (https://pubs.usgs.gov/of/1997/ofr-97-470/OF97-470C/index.html).

Geology of Nepal (from partners).

Earthquakes (http://www.seismonepal.gov.np/index.php?action=earthquakes&show=past).

2.7 Climatology and mereology

Metereological data from world clim with 19 variables and 3 mounthly averaged products for precipitation, wind and epapotranspiration at 1Km spatial resolution. (http://worldclim.org/version2).

Meteoreological data EMCF for the tropospheric correction (European Centre for Medium-Range Weather Forecasts) which works well with the TRAIN software.

Weather station for precipitation (Meteo office Nepal).

GIS and remote sensing softwares

ArcGIS (https://www.arcgis.com/features/index.html): proprietary software which reads the maps from the publication “Geology of Nepal”, used for geoprocessing of vector files in order to calculate with “field calculator” V_{SLOPE} and used for the layout and publication of maps.

GRASS GIS (https://grass.osgeo.org/): useful for semi-automatic extraction of river, watershed and with external plug in to calculate the geomorphon layer (useful for the identification of possible areas susceptible to shallow landslides) literature and the skyview factor (useful for the delineation and identification of deep seated slope deformation).

QGIS (https://www.qgis.org/en/site/) : alternative open source version of ArcGIS, and enriched with component from SAGA (useful software for file conversion and DEM manipulation), Orfeo (very powerful remote sensing software), together with several interesting Python plug-in such as:

“PS time series viewer”, automatic plotter;

“tile map scale level” open street map overlay;

“GEarthview” direct publication on google-earth of QGIS layout;

“semi-automatic classification plug-in” (for optical data classification such as Sentinel-2, TERRA-Aster and Landsat);

“vector field render”;

“magnetic declination” used for the orientation of the corner reflectors in the field.

Google Earth Pro (https://www.google.com/intl/en/earth/) : free software for the visualization in 2D and 3D of several generation optic images (proprietary) and the creation/overlay of raster/vector layers created in GIS and remote sensing software.

SNAP (http://step.esa.int/main/toolboxes/snap/): the ESA reference3 software for Sentinel-1, Setinel-2 and ENVISAT, ERS processing.

Adore-DORIS and DORIS (http://doris.tudelft.nl/): where the initial step of the interferometric chain start (it is suitable for ERS 1/ 2, Envisat, Terra-SAR-X, Alos, Radarsat, CosmoSkyMed).

Data ressources, processing platforms and applied software

StaMPS (https://homepages.see.leeds.ac.uk/~earahoo/stamps/): it is the most common open source software for PSI and SBAS time series analysis and work well in combination with DORIS, SNAPHU (unwrapping software), TRAIN (tropospheric correction software) and MATLAB.
MATLAB: proprietary software where the final steps of the stamps time-series processing.
G-POD (https://gpod.eo.esa.int/): analysis of ENVISAT performed but did not succeeded due to the lack of large archive of images.
Geohazard-TEP (https://geohazards-tep.eo.esa.int/#!): could be used in the future for the analysis of Sentinel-1 images.
GACOS (http://ceg-research.ncl.ac.uk/v2/gacos/) Generic Atmosferic Correction Online service for InSar could be used in the future couple with the liSC (http://comet.nerc.ac.uk/COMET-LiCS-portal/)portal for analysis of DInSAR.

References and relevant literature

ASTER GDEM (2018) https://asterweb.jpl.nasa.gov/gdem.asp . Last accessed 08 February 2018.

Bardi F, Frodella W, Ciampalini A, Bianchini S, Del Ventisette C, Gigli G, Fanti R, Moretti S, Basile G, Casagli N (2014) Integration between ground based and satellite SAR data in landslide mapping: The San Fratello case study. Geomorphology 223(2014):45–60

Berardino, P., G. Fornaro, R. Lanari, and E. Sansosti (2002), A new algorithm for surface deformation monitoring based on small baseline differential SAR interferograms, IEEE Trans. Geosci. Remote Sens., 40(11), 2375–2383

Bianchini S, Cigna F, Righini G, Proietti C, Casagli N (2012) Landslide hotspot mapping by means of persistent scatterer interferometry. Environ Earth Sci 67:1155–1172

Cascini L, Fornaro G, Peduto D (2010) Advanced low- and full-resolution DInSAR map generation for slow-moving landslide analysis at different scales. Eng Geol 112(1–4):29–42. doi:10.1016/ j.enggeo.2010.01.003

Cascini L, Peduto D, Pisciotta G, Arena L, Ferlisi S, Fornaro G (2013) The combination of DInSAR and facility damage data for the updating of slow-moving landslide inventory maps at medium scale. Nat Hazards Earth Syst Sci 13:1527–1549. doi:10.5194/ nhess-13-1527-2013.

Cigna F, Del Ventisette C, Liguori V, Casagli N (2011) Advanced radar-interpretation of InSAR time series for mapping and characterization of geological processes. Nat Haz Earth Syst Sci 11:865– 881

Cigna F, Bateson BL, Jordan CJ, Dashwood C (2014) Simulating SAR geometric distortions and predicting persistent scatterer densities for ERS-1/2 and ENVISAT C-band SAR and InSAR applications: nationwide feasibility assessment to monitor the landmass of Great Britain with SAR imagery. Remote Sens Environ 152:441–466

Colesanti C., and Wasowski J.(2006): Investigating landslides with space-borne Synthetic Aperture Radar (SAR) interferometry - Engineering Geology 88 (2006) 173–199.

CORINE—Copernicus Land Monitoring Services (2018) http://land.copernicus.eu/pan-european/corine-land-cover . Last accessed 08 February 2018.

DeCelles P., Robinson D., Quade J., Ojha T.P., Garzione C.N., Copeland P. and Upreti B.N. (2001) Stratigraphy, structure, and tectonic evolution of the Himalayan fold-thrust belt in western Nepal. Tectonics, Vol. 20, No. 4, Pg. 487-509, August 2001.

Dithal M.R. (2015) Geology of the Nepal Haimalaya –Regional Prespective of the Classic Collided Orogen. Regional geology Reviews. Springer. 2015.

European Centre for Medium-Range Weather Forecasts (2018) https://www.ecmwf.int/. Last accessed 08 February 2018.

ESA Radar Course (2018) https://earth.esa.int/web/guest/missions/esa-operational-eo-missions/ers/instruments/sar/applications/radar-courses/content-2/-/asset_publisher/qIBc6NYRXfnG/content/radar-course-2-slant-range-ground-range. Last accessed 08 February 2018.

Farina P, Colombo D, Fumagalli A, Marks F, Moretti S (2006) Permanent scatterers for landslide investigations: outcomes from the ESA-SLAM project. Eng Geol 88:200–217

Ferretti, A., et al., (1999): Permanent scatterers in SAR interferometry. International Geoscience and Remote Sensing Symposium, Hamburg, Germany, 28 June–2 July, 1999.

Ferretti, A., C. Prati, and F. Rocca (2001), Permanent scatterers in SAR interferometry, IEEE Trans. Geosci. Remote Sens., 39(1), 8 –20.

Ferretti A., et al., (2007): TM-19- InSAR Principles: Guidelines for SAR Interferometry Processing and Interpretation- ESA Publications, The Netherlands.

Garthwaite M., Nancarrow S., Hislop A., Thankappan M., Dawson, J. H. and Lawrie, S. (2015b). The Design of Radar Corner Reflectors for the Australian Geophysical Observing System: a single design suitable for InSAR deformation monitoring and SAR calibration at multiple microwave frequency bands. Record 2015/03. Geoscience Australia, Canberra. http://dx.doi.org/10.11636/Record.2015.003

Garthwaite M., Lawrie S., Dawson, J. H. and Thankappan M. (2015a) Corner Reflectors as the tie between InSAR and GNSS measurements: Case Study of Resource Extraction in Australia. Proc. 'Fringe 2015 Workshop', Frascati, Italy 23–27 March 2015 (ESA SP-731, May 2015).

References and relevant literature

Herrera G, Notti D, García-Davalillo JC, Mora O, Cooksley G, Sanchez M, Arnaud A, Crosetto M (2010) Analysis with C- and X-band satellite SAR data of the Portalet landslide area. Landslides.

Herrera G, Gutierrez F, Garcıa-Davalillo J, Guerrero J, Notti D, Galve J, Fernandez-Merodo J, Cooksley G (2013) Multi-sensor advanced DInSAR monitoring of very slow landslides: the Tena Valley case study (Central Spanish Pyrenees). Remote Sens Environ 128:31–43

Hoffmann J., Huber M., Marschalk U., Wendleder A., Wessel B., Bachmann M., Bräutigam B., Busche T., Hueso González J., Krieger G., Rizzoli P., Eineder M., and Fritz T. (2016) TanDEM-X Ground Segment DEM Products Specification Document. EOC – Earth Observation Center.

Hooper A., Zebker H., Segall P. and Kampes B (2004) A new method for measuring deformation on volcanoes and other natural terrains using InSAR persistent scatterers. Geophysical research letters, VOL. 31, L23611, doi:10.1029/2004GL021737, 2004.

Hooper A. and Zebker H (2007a) Phase unwrapping in three dimensions with application to InSAR time series. Vol. 24, No. 9/September 2007/J. Opt. Soc. Am. A.

Hooper A., Segall P. and Zebker H. (2007b)Persistent scatterer interferometric synthetic aperture radar for crustal deformation analysis, with application to Volcan Alcedo, Galapagos. Journal of Geophysical Research, VOL. 112, B07407, doi:10.1029/2006JB004763, 2007.

Hooper A. (2008) A multi-temporal InSAR method incorporating both persistent scatterer and small baseline approaches. Geophysical research letters, VOL. 35, L16302, doi:10.1029/2008GL034654, 2008.

Hungr O., Leroueil S., and Picarelli L., (2014), The Varnes classification of landslide types, an update, Landslide (2014) 11: 167-194.

Lesson 8: Radar and Microwave Remote Sensing (2018) http://wgbis.ces.iisc.ernet.in/envisrs/?q=node/39/. Last accessed 08 February 2018.

López-Dekker P., (2010): Introduction to SAR II: Acquisition modes, Applications, and future trends. ESA SAR Course.

Kampes B.M., (2006): RADAR INTERFEROMETRY- Persistent Scatterer Technique, German Aerospace Center by (DLR), Germany.

Meisina C, Zucca F, Notti D, Colombo A, Cucchi A, Savio G, Giannico C, Bianchi M (2008) Geological interpretation of PSInSAR data at regional scale. Sensors 8:7469–7492

Micheoud C., Abellan A., Derron M., and Jaboyedoff M., (2010) Safeland –Deliverable 4.1 – Review of Techniques for Landslide Detection, Fast Characterization, Rapid Mapping and Long-Tem monitoring.

Monitoring the Earth Deformation from Space (2018) http://vldb.gsi.go.jp/sokuchi/sar/qanda/qanda-e.html. Last accessed 08 February 2018.

Notti D, Davalillo J, Herrera G, Mora O (2010) Assessment of the performance of X-band satellite radar data for landslide mapping and monitoring: upper Tena Valley case study. Nat Haz Earth Syst Sci 10:1865–1875

Novali F. (2011) SAR Sensors Acquisition Geometries. The Interferometric Concept. TRE ltd.

Notti D., Herrera G., Bianchini S, Meisina C., García-Davalillo JC. and Zucca F. (2014) A methodology for improving landslide PSI data analysis. Int J Remote Sens 35(6)

Ofori N. Pearson and Peter G. DeCelles (2005) Structural geology and regional tectonic significance of the Ramgarh thrust, Himalayan fold-thrust belt of Nepal. Tectonics, Vol. 24, TC4008, doi:10.1029/2003TC001617, 2005

PanGeo PSI training in Rome in October 2011 (2018) http://www.pangeoproject.eu/eng/educational. Last accessed 08 February 2018.

pyrocko.org - Software for Seismology (2018) https://pyrocko.org/. Last accessed 08 February 2018.

Richards J.A., (2009): Remote Sensing with Imaging Radar. Springer-Verlag Berlin Heidelberg 2009.

Righini G, Pancioli V, Casagli N (2011) Updating landslide inventory maps using persistent scatterer interferometry (PSI). Int J Remote Sens 33(7), 2012

Robinson D., DeCelles P. and Copeland P. (2006) Tectonic evolution of the Himalayan thrust belt in western Nepal: Implications for channel flow models. GSA Bulletin; July/August 2006; v. 118; no. 7/8; p. 865–885; doi: 10.1130/B25911.1.

References and relevant literature

Sandwell D., et al., (2011): GMTSAR: An InSAR Processing System Based on Generic Mapping Tools - Scripps Institution of Oceanography Technical Report, Scripps Institution of Oceanography, UC San Diego.

Strozzi T., et al., (2001): Land Subsidence Monitoring with Differential SAR Interferometry - Photogrammetric Engineering & Remote Sensing. Vol. 67, No. 11, November 2001, pp. 1261-1270.

Toolbox for Reducing Atmospheric InSAR Noise (2018) http://davidbekaert.com/ . Last accessed 08 February 2018.

Vecchiotti F., Peduto D. & Strozzi T. (2017a): Multi-sensor a Priori PSI Visibility Map for Nationwide Landslide Detection in Austria - Springer International Publishing AG 2017 - M. Mikoš et al. (eds.), Advancing Culture of Living with Landslides, DOI 10.1007/978-3-319-53498-5_6.

Vecchiotti F., Peduto D. & Strozzi T. (2017b): Multi-sensor a Priori PSI Visibility Map for Nationwide Landslide Detection in Austria – Presentation at the 4th World Landslide Forum, Ljubljana.

Wasowski J, Bovenga F (2014) Investigating landslides and unstable slopes with satellite multi temporal interferometry: current issues and future perspectives. Eng Geol 174:103–138

Wegmüller U. and Werner C. (2010) PSI Precision, accuracy and validation aspects. Terraferma Users Training 2-Dec-2010.

Zebker, H., Shankar P. and Hooper A. (2007) InSAR Remote Sensing Over Decorrelating Terrains: Persistent Scattering Methods. IEEE 1-4244-0284-0/07/